Journal of Structural Geology, Vol. 7, No. 5, pp. 613 to 620, 1985
Printed in Great Britain

0191-8141/85 $03.00 + 0.00

Low-angle normal faults in Lower Eocene chalks near Beer Sheva, Israel

Dov Bahat

Department of Geology and Mineralogy, The Ben Gurion University of the Negev, Beer-Sheva 84-105, Israel

(*Received* 4 *July* 1984; *accepted in revised form* 27 *January* 1985)

Abstract—Forty outcrops of Lower Eocene chalks (Mor Formation) around Beer Sheva were examined for faulting. Ten well-exposed normal faults, with mean dip and strike of 39 ± 6° and 294 (N66°W) ± 28°, respectively, were found in four outcrops. The timing of fault movement is partly constrained by unfractured Lower Eocene chert nodules which follow some of the fault traces. Hence, the faults are interpreted to be the result of dynamic failure due to horizontal NNE–SSW compression during the Early Eocene. Horizontal compression is implied by analogy to descriptions of recent faulting caused by an earthquake in another location, local folding in the Lower Eocene, secondary fractures and flat and ramp structures associated with the investigated faults.

INTRODUCTION

Eocene rocks (Bentor & Vroman 1963, Braun 1967) were deposited mainly within structural downwarps between the anticlines of the Syrian Arc, formed at various times since the Santonian. The present study concerns low-angle (<45°) normal faults in chalks of the Mor Formation (Lower Eocene) in the southern part of the Shephela syncline north of Beer Sheva, and the northern part of the Beer Sheva syncline to the south, both areas being situated in a rhomb area defined by diagonals of some 47 km × 30 km (Figs. 1 and 2). The investigation of faulting has been carried out as a part of a wider project which included a study of various aspects of fracture in these chalks (Bahat 1983, in press).

Previous studies of low-angle normal faults are mostly related to structures of crustal or lithospheric dimensions (e.g. Wernicke 1981). Published information on low-angle faulting in chalks is limited and this investigation presents data on such faults of outcrop scale.

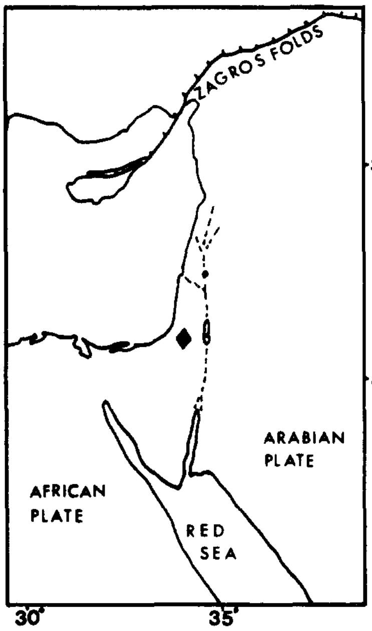

Fig. 1. Location map. The investigated area is the diamond-shaped rhomb at the centre of map.

PRECISION OF MEASUREMENTS

All the dip and strike readings reported in Table 1 were taken by the writer and most were checked by students. Deviations for individual dips are generally considered to be ±5°. Deviations for strikes are ±7°, but these are reduced to ±3° for strikes of faults 1, 1a, 2 and 2a in outcrop A (where the same normal faults continue across the road).

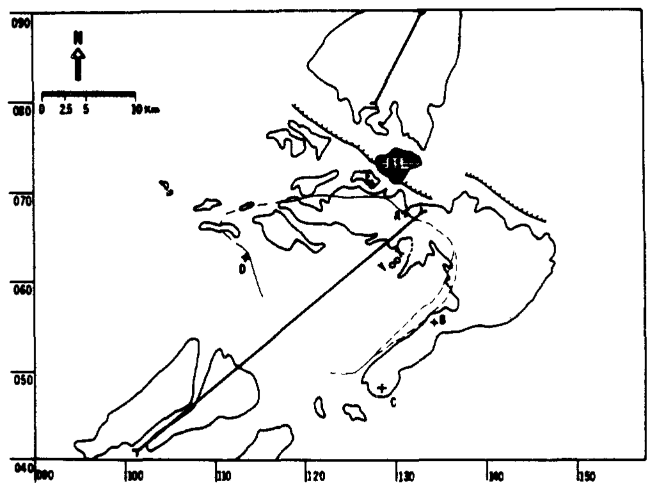

Fig. 2. Five outcrops marked by a + sign and designated by A–E in the investigated area. Joints and en échelon fractures occur at locations X and Y (see Bahat in press). Heavy lines are boundaries of Eocene after Bentor *et al.* (1970), fine lines are boundaries between the Mor and Horsha Formations, barbed lines are inferred faults south of Beer Sheva (BS) after Gvirtzman (1969).

LOW-ANGLE NORMAL FAULTS

Fractures in forty outcrops were examined and normal faults were found in only five (Fig. 2), one of which contained a fault unsuitable for measurement. The observations are summarized in Table 1 according to the

Table 1. Field data from low-angle normal faults in Lower Eocene chalks near Beer Sheva

Outcrop	Fault number	Dip (degrees) and dip direction (degrees)	Strike (degrees)	Throw (cm)	Extension (cm)	Mineralization	Special features
A	1	33/194	284	?	?	chert	secondary fracture dips 53° two secondary fractures dip 90°
	1a	35/194	284	120	171	chert	secondary fracture dips 49° flat and ramp structure
	2	38/024	294	80	102	chert	two shear planes
	2a	39/024	294	40	49	chert	secondary fracture dips 45–61°
	3	34/010	280	10	15	chert	
	4	36/180	270	90	124		
B	5	*55/236	*326	15	10		flat and ramp structure, dip varies between 38 and 80°, strike varies between 315 and 338°
	6	42/055	325	80	89		
	7	45/235	*325	100	100		strike varies between 308 and 342°
C	8	33/230	320	50	77	calcite	wedging due to folding
D	9	38/180	270	20	26	chert plate	fault terminates at lower part of outcrop
	10	39/153	243	60	74		

Extension (e) is a function of the throw (t) and dip (θ) according to $t/e = \tan\theta$ (Wernicke & Burchfiel 1982).
*Mean of measurements at four locations.

individual outcrops, and outcrop A is characterized below in some detail. Bedding is approximately horizontal in most exposures with the exception of outcrop C which is moderately folded. Throws and extensions of individual faults are generally below 1.75 m.

Outcrop A

Two parallel exposures (29 m apart) are divided by a N–S road (from Beer Sheva to Nizzana). There are four low-angle normal faults along the eastern exposure (1–4, Table 1), and only the traces of the two southern faults (1a and 2a, Table 1, respectively) are also observable in the western exposure. The implication is that fault lengths are at least several tens of metres. All the faults in this outcrop which attains a maximum height of 6 m cut the entire exposure.

The two southern faults (1 and 2) are only 28 m apart and have similar strikes and dips. The faults are 65 m away from the other two faults (3 and 4) which also yield similar attitudes. Faults 1 and 2 dip away from each other and display similar amounts of throw. They seem to represent a set which reflects the same palaeo-stress phase and are considered to be conjugate faults (Fig. 3a). The two northern faults also appear to be a consequence of the same stress episode (Fig. 4).

Chert nodules form horizontal 'trains' and alternate with chalk beds throughout the Mor Formation. Such nodules occur along fault planes 1–3 measured in outcrop A (Fig. 3b, Table 1). Nodules are particularly well exposed in fault 2 where they are only slightly fractured, implying that faulting occurred mostly before complete consolidation of the chert. That is, faulting probably occurred in the Early Eocene. No chert occurs at higher stratigraphic levels in the area (the Horsha Formation of the Middle Eocene). It should, however, be added that in fault 1a chert is more intensely fractured than in fault 2, implying that the latest offsets occurred when the chert was already considerably consolidated.

Secondary structures

A special structural feature that repeats itself in several exposures (Table 1) is a system of secondary fractures adjacent to the low-angle faults. The fractures are manifested by cracks that branch from the main fault. Initially, branching is with a steep dip upward, but its continuation may be subparallel to the parent fault, or at an acute angle to it. In fault 2, the secondary crack propagates some metres before joining back into the fault (Fig. 3a). Separate offsets occur along the two subparallel planes which result from this propagation. In fault 1 the entire offset is along the low-angle fault plane. There are three secondary fractures that branch from the fault, one dips at 53° and the other two are almost vertical. Hence, a radiation of three secondary fractures from the same location occurs along the fault (Fig. 5a). Fault 1a is curved into a flat and ramp pattern and a single crack branches upward from the main fault at a dip of 49°. Branching was initiated along the ramp. The flat occurs along the bed boundaries (between chert and chalk). In faults 1 and 2 fault branching stems from a location along the fault plane and not at the end of the main shear as observed by Chinnery (1966).

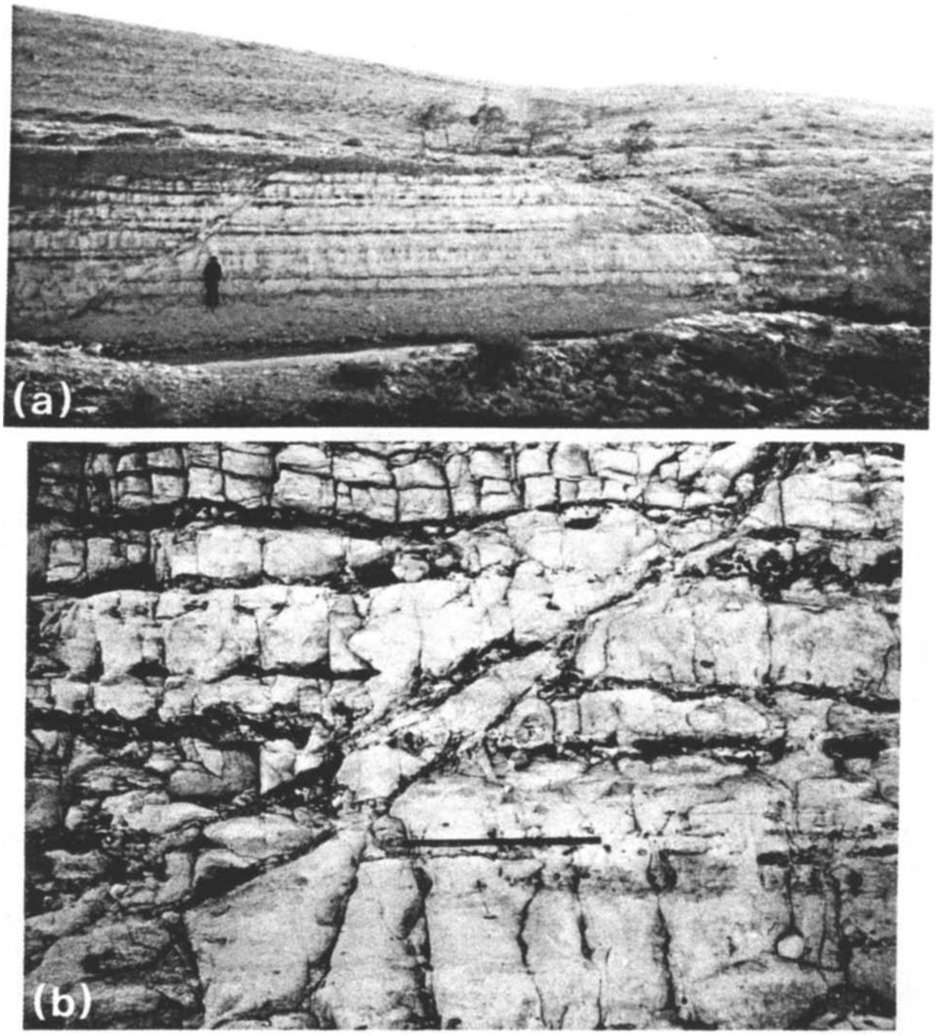

Fig. 3. Faults in outcrop A. (a) Two conjugate faults, fault 1 on the right and fault 2 on the left (near the man). (b) Fault 2, dark chert nodules are seen as horizontal beds and along the two dipping fault planes. The ruler is 90 cm long.

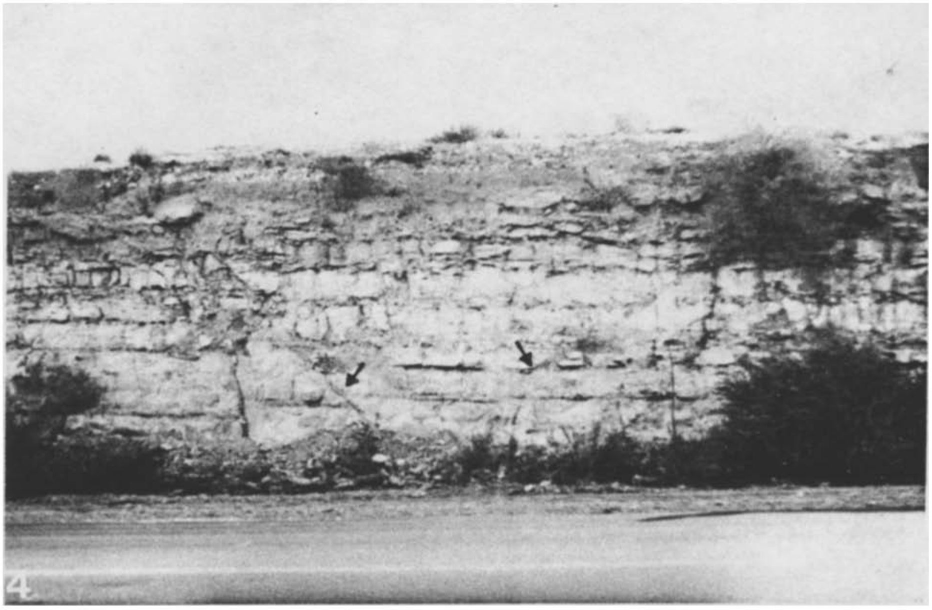

Fig. 4. Outcrop A. Fault 3 (right-hand arrow) and fault 4 (left-hand arrow) (Table 1). Typical thickness of beds in this exposure is 0.5 m.

Fig. 6. Fault 9 in outcrop D (Table 1). An unfractured chert plate is observed along the fault plane. Scale near the plate is 15 cm.

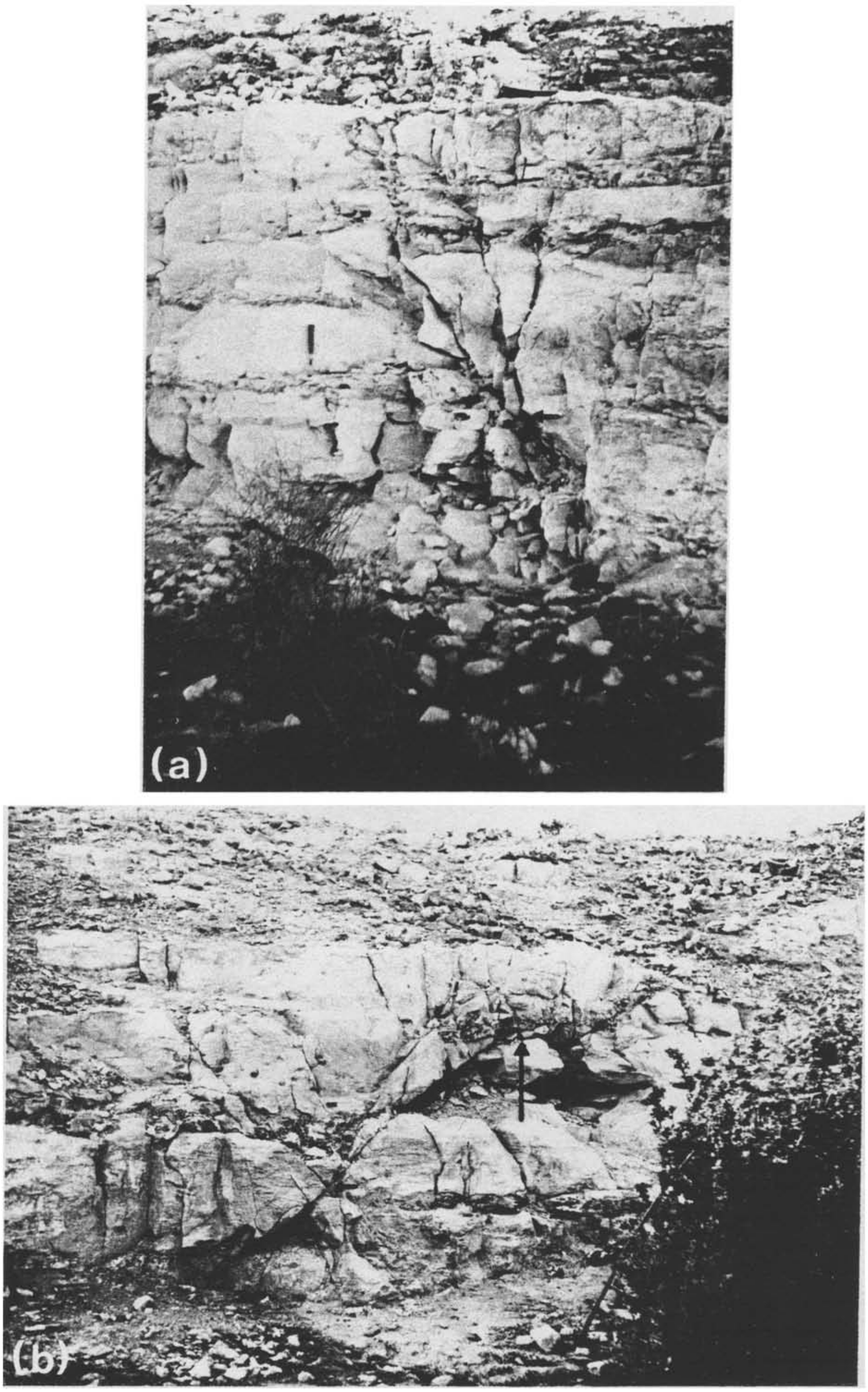

Fig. 5. Fault 1 in outcrop A. (a) Fault 1 on the eastern side of the road. Four branches of the fault can be distinguished. The two on the left dip (clockwise) 33 and 53°, respectively (the latter is more clearly visible than the former). Additionally, there are two subvertical branches that stem together with the 53° dipping branch from the same location. Hammer is 30 cm long. (b) Fault 1a (on the western side of the road) is branched (clockwise) into 49 and 35° dipping branches. Locations of branching are marked by short arrows. The low dipping plane has the structure of a flat (below a chert bed marked by a long arrow) and ramps. Ruler is 30 cm long.

Other outcrops

In outcrop B, fault 6 is 36 m east of fault 5, and 150 m west of fault 7. The mean strikes of the three faults are almost identical. Fault 5 is curved and shows considerable variations in both strike and dip (Table 1). This is the only high-angle (>45°) normal fault found in the investigated area. Fault 7 shows variations in strike but is of uniform dip (Table 1). On the northern side of outcrop C, a chalk layer wedges out at the upper part of the outcrop. This probably is a consequence of folding during the Lower Eocene. A striking feature of fault 9 in outcrop D is the presence of a totally unfractured plate of chert with uniform thickness (about 0.8 cm) along the fault plane (Fig. 6). This fault abruptly terminates in the lowest 3 m of the outcrop which is 17 m high. The implication is that the fault did not even extend into the Lower Eocene rocks above. The presence of the chert plate along the fault suggests that it was formed when the normal fault had already achieved its present shape (see fault 2 above). A low-angle fault was observed in outcrop E, but its poor exposure precluded its use in this study.

Summary of observations

The mean dip of ten well-exposed faults is 39 ± 6°. With the exception of one fault (1) the normal sense of offset was established in the field. The mean strike of the ten faults is 294 ± 28°. The faults generally appear in groups of 2–4 faults in a limited number of outcrops. Perhaps more than two faults constitute a conjugate set in outcrops A and B. The stress system which resulted in this faulting was operative in the Early Eocene.

DISCUSSION

The low-angle normal faults were probably initiated when the maximum principal stress was horizontal and normal to the present strike of the faults and the minimum principal stress was vertical. Normal displacements probably occurred when the horizontal stresses near the surface relaxed (Ambraseys 1981). A comparable situation was described by King & Vita-Finzi (1981) in their analysis of the Algerian earthquake of 10 October 1980. An earthquake, caused by horizontal compression, was associated with faulting that reached the surface. These authors observed that although reverse faulting was clear and unambiguous in the investigated area, the most extensive and striking features of the surface deformation were normal faults and other tensional features (Fig. 7a). Hence, dynamic failure due to horizontal compression can be manifested close to the surface as normal faulting. This mechanism is interpreted to be the possible cause for the normal faults in the Lower Eocene chalks of Beer Sheva. Reverse faults have not been identified in the investigated synclines, but Gvirtzman (1969) on the basis of geophysical data and information from several drill holes south of Beer Sheva has inferred buried sinistral faults striking WNW

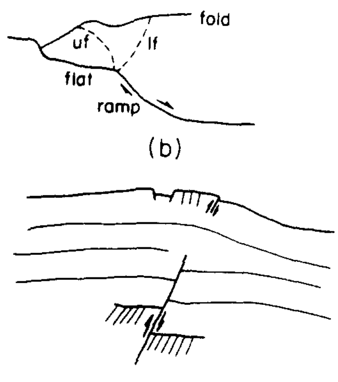

Fig. 7. Hypothetical sections. (a) An antiformal fold above a thrust in the basement. Reverse and normal faults as well as vertical fractures occur at the surface (modified after De Sitter 1962 and King & Vita-Finzi 1981). (b) Fault with flat and ramp on footwall and with fold in hangingwall. Antithetic faults develop in hangingwall in response to loading (lf) and unloading (uf) at ramp (modified after Gibbs 1984, fig. 9a).

(Fig. 2). Also, Letouzey & Trémolières (1980) and Eyal & Reches (1983) studied mesostructures in Late Cretaceous to Miocene rocks in various parts of Israel (and Sinai). They concluded that their results demonstrated WNW–ESE compression, which is the direction of the present mean strike of the investigated faults.

The presence of the fault displaying a flat and ramp structure (faults 1a and 5) and secondary fractures, radiating from impingement points along the curving fault (Fig. 5a), resembles a model for a listric fault with a flat and ramp and an antithetic fault developed in its hangingwall (Gibbs 1984, figs. 5a, 9a). Conditions of loading and unloading at the impingement point (on the ramp) would possibly dictate variations in angular relationships (Lawn & Swain 1975) between the footwall and secondary fractures (Fig. 7b).

Folds of 150 m wavelength in Lower Eocene rocks in the area and the wedging of chalk in outcrop C, imply horizontal compression. These structures are analogous to compressional folds associated with extensional faults as observed by Ambraseys (1981) and King & Vita-Finzi (1981).

Acknowledgements—This study was supported by the Ministry of Energy and Infrastructure Earth Science Research Administration. I thank Beni Rophe, Yuval Winter and other students for their help in the field work. This paper benefited from some critical reading by B. P. Kohn.

REFERENCES

Ambraseys, N. N. 1981. The El Asnan (Algeria) earthquake of 10 October 1980, conclusions drawn from a field study. *Q. Jl Engng Geol. Lond.* **14**, 143–148.

Bahat, D. 1983. Jointing in Lower Eocene rocks of the Northern Negev. *Israel Geol. Soc. Ann. Meet. Abstr.*, 4–5.

Bahat, D. in press. Joints and en échelon cracks in Middle Eocene chalks near Beer Sheva. *J. Struct. Geol.*

Bentor, Y. K. & Vroman, A. 1963. The geological map of Israel 1:100,000 sheet 17, Nizzana. *Geol. Surv. Isr.*

Bentor, Y. K., Vroman, A. & Zak, I. 1970. Geological Map, Israel 1:250,000, southern sheet. *Surv. Isr.*

Braun, M. 1967. Type sections of Avedat group, Eocene formations in the Negev (Southern Israel), *Geol. Surv. Isr., Strat. sect.* **4**, 1–14.

Chinnery, M. A. 1966. Secondary faulting—I. Theoretical aspects. *Can. J. Earth Sci.* **3**, 163–174.

De Sitter, L. U. 1962. Structural development of the Arabian Shield in Palestine. *Geologie Mijnb.* **41**, 116–124.

Eyal, Y. & Reches, Z. 1983. Tectonic analysis of the Dead Sea Rift region since the Late Cretaceous based on mesostructures. *Tectonics* **2**, 167–185.

Gibbs, A. D. 1984. Structural evolution of extensional basin margins. *J. geol. Soc. Lond.* **141**, 609–620.

Gvirtman, G. 1969. The Saqiye Group (Late Eocene to Early Pleistocene) in the Coastal Plain and Hashephela regions, Israel. *Bull. geol. Surv. Isr.* **51** (2), Map 8.

King, G. C. P. & Vita-Finzi, C. 1981. Active folding in the Algerian earthquake of 10 October 1980. *Nature, Lond.* **292**, 22–26.

Lawn, B. R. & Swain, M. V. 1975. Microfracture beneath point indentations in brittle solids. *J. Mater. Sci.* **10**, 113–122.

Letouzey, J. & Trémolières, P. 1980. Paleo-stress fields around the Mediterranean since the Mesozoic derived from microtectonics: comparisons with plate tectonic data. *26th Int. Geol. Congr. Paris, Colloq.* **C-5**, 261–273.

Wernicke, B. 1981. Low-angle normal faults in the Basin and Range province: nappe tectonics in an extending orogen. *Nature, Lond.* **291**, 645–648.

Wernicke, B. & Burchfiel, B. C. 1982. Modes of extensional tectonics. *J. Struct. Geol.* **4**, 105–115.